

UTIS AC 83-50

X-651-72-457

PREPRINT

NASA TM-X-66130

AN EXTREME ULTRAVIOLET PHOTOMETER FOR SOLAR OBSERVATIONS FROM THE ATMOSPHERE EXPLORER SATELLITES

DONALD F. HEATH
JOHN F. OSANTOWSKI

(NASA-TM-X-66130) AN EXTREME ULTRAVIOLET
PHOTOMETER FOR SOLAR OBSERVATIONS FROM
THE ATMOSPHERE EXPLORER SATELLITES D.F.
Heath, et al (NASA) Dec. 1972 30 p

N73-13437

Unclas
CSCL 20F G3/14 50225

DECEMBER 1972



— GODDARD SPACE FLIGHT CENTER —
GREENBELT, MARYLAND

AN EXTREME ULTRAVIOLET PHOTOMETER FOR SOLAR
OBSERVATIONS FROM THE ATMOSPHERE EXPLORER SATELLITES

Donald F. Heath
Meteorology Branch

John F. Osantowski
Optics Branch

GODDARD SPACE FLIGHT CENTER
Greenbelt, Maryland 20771

PRECEDING PAGE BLANK NOT FILMED

**AN EXTREME ULTRAVIOLET PHOTOMETER FOR SOLAR
OBSERVATIONS FROM THE ATMOSPHERE EXPLORER SATELLITES**

**Donald F. Heath
Meteorology Branch**

**John F. Osantowski
Optics Branch**

ABSTRACT

A broad band photometer experiment is being fabricated for the Atmosphere Explorer C, D and E missions to record the solar irradiance in the 40 to 1250Å region with seven distinct passbands. The experiment consists principally of four spinal electron multipliers located behind a moving eight position filter wheel. Six metallic filters are used to spectrally isolate the solar irradiance. In addition three Al_2O_3 diodes, two with filters, are being used to record the solar irradiance over the range of orbital altitudes from perigee through apogee. A principal goal of the experiment will be to measure time dependence of the solar irradiance with respect to a storage ring synchrotron light source which has been calibrated in terms of the best currently available standards of irradiance.

Preceding page blank

PRECEDING PAGE BLANK NOT FILMED

CONTENTS

	<u>Page</u>
Abstract	iii
Introduction	1
Instrument Description	2
<u>Mechanical</u>	2
Optical	3
<u>Calibration</u>	6
Electrical	8
<u>Geophysical Data</u>	10
Summary	12
References	13

TABLE

<u>Table</u>	<u>Page</u>
1 The ESUM Filters and the Wavelength Response Band for 50% of the Signal Are Given	14

ILLUSTRATIONS

<u>Figure</u>		<u>Page</u>
1	ESUM Experiment	15
2	Transmittance for the 1730A thick In - 1% Ti alloy filter shown here is comparable to a Sigmatron pure In filter of similar thickness.	16
3	Comparison of the transmittances for a pure Sn filter (1600A thick) and a Sn - 3% Ge (1700A thick) alloy filter. The alloy filter exhibits superior resistance to moisture attack.	17
4	Transmittance for a standard sigmatron Al - 1% Si alloy filter 1800A thick.	18
5	Transmittance for a 1000Å thick pure Ti filter which was pin-hole free but not opaque to visible radiation.	19
6	Calculated response of typical ESUM photometer channels using published filter transmittance curves and the NBS Al ₂ O ₃ standard diode quantum efficiency curve depicted in Figure 7. ...	20
7	Quantum efficiency of NBS, Al ₂ O ₃ standard diode. The broken curve below 600A is an extrapolation some preliminary measurements (made at Ball Bros. Res. Corp.) indicate a plateau in quantum efficiency between 500A and 200A.	21

ILLUSTRATIONS (Continued)

<u>Figure</u>		<u>Page</u>
8	The function $F(y) \propto \frac{\partial^2 P}{\partial \lambda \partial \psi}$ is the spectral distribution function where $y = \lambda c / \lambda$ and is used in the calculation of the emitted power per unit wavelength and angle.	22
9	Spectral energy distribution for a 250 MeV, one milliamperere beam into one milliradian. The succeeding smaller curves are for decreases in energy in increments of 10 MeV.	23

AN EXTREME ULTRAVIOLET PHOTOMETER FOR SOLAR OBSERVATIONS FROM THE ATMOSPHERE EXPLORER SATELLITES

Introduction

The solar extreme ultraviolet (EUV) irradiance is a quantity of major importance in the mission objectives of the Atmosphere Explorer (AE) Program. Atmospheric absorption of solar EUV radiation (40-1250A) which is a major source of heat and ionization in the 100 to 250 km region of the atmosphere. It is this altitude regime which will be explored in great detail by "in situ" measurements on board the AE spacecraft.

The extreme solar ultraviolet monitor (ESUM) experiment is a broadband (halfwidth of a few 100A) multichannel photometer experiment which is designed to investigate the magnitude and the nature of the variability of the solar irradiance in the 40 to 1220A region in seven channels over the operational lifetime of the satellite. The wavelength selectivity of the detector channels is determined by the wavelength pass band of thin metallic filters whose thicknesses are measured in hundreds to thousands of angstroms and the variation of detector quantum efficiency with wavelength. Examples of some typical filter transmittances, a discussion of their transmittances, and an extensive bibliography on the subject can be found in the review work by Samson (1967).

Two types of photoelectric detectors are being used, Spiraltron electron multipliers (SEM's by Bendix) and windowless, opaque photocathode, diodes (EMR). The former possess high sensitivity to low light levels while the latter exhibit very high signal stability for intense radiation sources. The operating range of the ESUM photometer is intermediate between the two extremes.

Consequently one system of detectors does not adequately fulfill the ESUM experiment requirements and hence both are used which in turn provides some redundancy.

There are two operating modes. One for spinning or 4 RPM mode where the filter wheel is stepped by a sun sensor or spacecraft nadir pulse and the other which is a free running mode where the filter wheel is stepped automatically every 16 seconds. Another operating data mode is having the high voltage and SEM's off with only the low voltage on and operating the EUV diodes. It is anticipated that the EUV diodes will be operated continuously whereas it is expected that an automatic high data rate shut down provision will turn off the high voltage through the apogee portion of the orbit due to the effects of the high energy trapped particle radiation background.

Instrument Description

Mechanical

The instrument is shown in Figure 1 and consists of two principal components: the detector head with its associated electronics and the main electronics box. The ESUM is located on the -Y axis and is pointed radially at an angle of 65° to the +Z axis and is sensitive over a 60° total field of view.

Mechanical restraints imposed on the experiment configuration for the reduction of scattered light require the occultation of the edge of the diode detectors for about 7° at the edge of the 30° half cone half angle field of view on the in-board side which passes through the optical axis.

The basic configuration consists of four channeltron electron multipliers (Bendix Spiraltrons) located behind an 8-position stepped filter wheel. The

filter wheel contains 6 metallic filters with transmission bands in the 40 to 1100A region, an Fe^{55} soft x-ray calibration source and a blank position to provide a zero light signal level. A visible light diode is also located behind the filter wheel in one of the detector positions to monitor the filter integrity and pinhole transmission throughout the course of the mission. Three windowless diodes with Al_2O_3 photocathodes are positioned beyond the edge of the filter wheel. Two of the photodiodes have fixed filters in front of the photocathode. A filter protection mask serves both to protect the filters during the launch and low perigee phases as well as to further reduce the level of scattered light reaching the detectors.

An experiment requirement that the scattered light level must be less than 1% of the signal level when the solar vector sweeps through the instrument field of view is satisfied by incorporating baffles into the protection mask and filter wheel. In order that the windowless or open detectors and the filters are not subjected to a severe contamination environment during prelaunch, the detector head will be launched sealed with a cover which will be ejected sometime during the second or third week in orbit.

Optical

The operational design goal of the AE experiments is for one year with a negligible change in instrument performance over that period. This is a very severe requirement for the optical experiments operating in the ultraviolet on a satellite which utilizes an on-board propulsion system to drop perigee below 150 km. This operation introduces both contamination and thermal problems. Apart from a change in their wavelength response characteristics from the

above, both filters and photodetectors are subject to other problems. The channel multipliers appear to have a finite or total accumulated count lifetime which seems to be independent of the count rate.

The metallic filter onset of transmission is predicted by the free-electron model of metals which states that at some critical frequency the metallic film will undergo a transformation from a reflecting to a transmitting medium. The electron plasma can support an electromagnetic wave for

$$\nu > \nu_P = \left(\frac{n e^2}{\pi m} \right)^{1/2} = 9 \times 10^3 n^{1/2}$$

where n is the number of electrons cm^{-3} that undergo collective oscillations. The electronic charge and mass are designated by e and m respectively. The inner electron absorption edges provide the short wavelength cut-off in the filter transmittance curve.

The filter foils supplied by Sigmatron Inc. are nominally about $0.16 \mu\text{m}$ thick and are supported on 70 line per inch nickel screens which exhibit a transmittance of about 90%. The two most potentially damaging environments to the metal filters on AE are corrosion by moisture in the prelaunch phase and thermal cycling due to atmospheric heating generated by low perigee passes. Appreciable humidity produces corrosion which is evidenced by the generation of pin holes. High humidity can increase the white light leakage of a filter by 10^4 in one day which in the AE ESUM experiment would constitute a catastrophic failure. The other filter problem arises when the foils are thermally cycled close to their melting point. This results in thermal recrystallization which is evident from an increase in white light pinhole transmittances. Unfortunately the filter choices

for AE are based on their optical transmission bands and not their thermal and mechanical properties. Two filters, indium and tin, have melting points of 157C and 232C and could cause problems during perigee passages. This problem may be alleviated through alloying. In the case of indium an alloy of 1% Ti, 99% In produced a filter whose transmission band essentially was unchanged from pure indium and which survived catastrophic failure up to 300C. At this temperature one probably has a liquid metal filter between two oxide films. The preceding data on the filter foils were obtained from the work of Steele and Reynolds (1972).

The wavelength passband of the response to the incident solar radiation is determined by the product of an angular response function, photocathode quantum efficiency, filter transmittance and the solar irradiance which lies inside the passband of the filter-detector response curve.

Examples of typical transmittance curves for four of the six filters which have been developed by Sigmatron Inc. are given in Figures 2-5 for In-Ti, Sn, Al and Ti respectively. The aluminum and aluminum plus carbon filters are a standard stock item hence they were not a part of the developmental effort. The carbon produces a short wavelength absorption which excludes the He 584A line. The aluminum plus parylene filter is for the spectral region of the sun below 100A and at the moment is questionable for the AE-C mission due to a lack of experimental data.

Using the solar irradiance data of Hinteregger (1970) and typical transmittance curves from Rustgi (1968) for the AE filters which are listed in Table 1, the channel response to the solar irradiance can be computed. This is shown graphically in Figure 6 where the normalized sum of the product of typical filter

transmittances (T_λ), photocathode quantum (Q_λ), and the solar irradiance (F_λ) from 0 to λ is shown as a function of wavelength; i.e.,

$$\sum_0^\lambda F_\lambda Q_\lambda T_\lambda / \sum_0^\infty F_\lambda Q_\lambda T_\lambda .$$

The photocathode quantum efficiency, Q_λ , for an NBS standard Al_2O_3 diode was used. It was provided by L. R. Canfield of the National Bureau of Standards and is shown in Figure 7 to illustrate the typical quantum efficiency of the diodes in the experiment. Due to insufficient experimental data on the transmittance for the aluminum plus parylene filter, data for aluminum plus mylar has been substituted. The broken curve, for the region below the peak in quantum efficiency is similar in shape to the typical quantum efficiency curves for channel electron multipliers which are essentially the same as the spiraltron electron multipliers (SEM) being used in this experiment. The extreme sensitivity of the spiral electron multipliers and the relatively high solar irradiance in the EUV make it necessary to attenuate the solar radiation before it reaches the photocathode of the SEM's. A typical reduction of the order of 1.3×10^{-4} is needed and is obtained using a neutral density screen at the channel of $T = 5 \times 10^{-2}$, an aperture at the filter of $5 \times 10^{-2} \text{ cm}^2$ and a neutral density screen on the solar side of the filter of $T = 5 \times 10^{-2}$. Unfortunately the solar irradiance is not large enough to use photodiodes behind the filters.

Calibration

The absolute radiation calibration is a three-step process. First the individual filter transmittances and detector quantum efficiencies will be measured as a function of wavelength. Secondly a system calibration will be performed

using synchrotron radiation as an absolute irradiance standard. The synchrotron radiation is a calculable quantity which depends upon the number of electrons in the storage ring, the beam energy, the magnetic field intensity and the electron orbit. This serves not only as a check on the component calibration but it represents a laboratory irradiance standard which can be referenced to the sun. Thirdly, the angular response functions will be performed in orbit by torquing the spacecraft through the 60° angular field of view of ESUM in 5° increments.

The source of synchrotron radiation to be used as a radiation standard for the ESUM calibration is the 240 MeV electron storage ring at the Physical Sciences Laboratory (PSL) of the University of Wisconsin. The PSL storage ring traps and accelerates a high energy electron beam for hours. In the normal operation the electrons circulate at a frequency of 32 MHz as a group which extends about 40 cm along the orbit.

The rms angular spread of the radiation cone perpendicular to the orbit measured from the orbital plane where $\gamma = E / M_0 c^2 <\psi^2>^{1/2} = \gamma^{-1} (\lambda / \lambda_c)^{1/3}$ which is of the order of 2×10^{-3} radians for 250 MeV electrons where $\lambda_c = 4 \pi R \gamma^{-3} / 3 = 216 \text{Å}$. For use as an absolute radiation standard one must know the instantaneous power per unit wavelength and angle which is given by:

$$\left. \frac{\partial^2 P}{\partial \lambda \partial \psi} \right|_{\psi=0} = \frac{3 n e^2}{\lambda_c^2} \gamma^2 F(y) \frac{\text{ergs}}{\text{cm}^2 \text{ sec Å rad}}$$

Where $y = \lambda_c / \lambda$

for the forward radiation γ
per radian in the orbital

$$F(y) = y^4 K_{2/3}^2(y/2) \quad \text{plane where } \psi = 0.$$

$$K_{2/3}(x) = \frac{\pi}{\sqrt{3}} \left[i^{2/3} J_{-2/3}(ix) - i^{2/3} J_{2/3}(ix) \right]$$

where J's are Bessel functions of imaginary argument.

The function F (y) is shown graphically in Figure 8. The preceding section on the synchrotron radiation is taken from the PSL Synchrotron Radiation Facility Users Handbook which is based upon the theoretical work by Schwinger (1949) and the work of Tomboulia and Hartman (1956).

The synchrotron radiation continuum in the EUV is essential for the measurement of the filter transmittances and the absolute system calibration. An example of a calculated spectral energy distribution for a 250 MeV, one milliamp beam is given in Figure 9 which is also from the PSL Synchrotron Radiation Facility Users Handbook.

Since there is some small uncertainty in the absolute value of the beam current, the absolute experiment calibration will be performed by comparing the synchrotron radiation intensity with a 1000 watt quartz iodine lamp standard of irradiance at 4000A where the recently developed QI irradiance standard is known to an absolute accuracy of 1.5%. This calibration of the synchrotron light at 4000A will then be used to compute the radiation intensity in the EUV based on the theoretical shape of the intensity distribution curve. The EUV radiation standard is then assumed to be known for the calibration of ESUM.

Electrical

The electronics of the ESUM basically consists of two parts: The first part utilizes a pulse counting system for the channel electron multipliers which are designed to operate at a nominal 10^4 Hz rate which is optimum from the standpoint

of providing a 1% statistical counting accuracy over 1 sec and at the same time not exceeding the nominal total accumulated count lifetime over one year. Each channel has its own counter and shift register for transferring the count out at 0.25 sec intervals. A single high voltage power supply is used with 4 commandable voltage levels to keep the SEM's operating in the pulse counting saturated mode. Output pulses from each of the SEM's go through a low level discriminator into their appropriate counters which are reset every 0.25 sec and transferred out to their shift register for transfer out to the spacecraft telemetry system.

The second section consists of an individual electrometer circuit for each of the 4 diodes, 3 EUV and one visible light. The electrometer circuit is composed of a current to voltage converter with a transresistance of 10^{10} ohms followed by a 7 range gain change amplifier with a maximum gain of 200 which is reduced by factors of two to a minimum of 3.16.

System resolution is limited by the A to D converter resolution and the electrometer noise level. With the 8 bit A to D converter and the present system, gain resolution is limited to approximately 1×10^{-14} A. System noise has been measured on a breadboard model to be 6×10^{-15} A peak-to-peak or approximately 1×10^{-15} A RMS.

System response time is set by a single R-C filter with a time constant of 80 ms. Gain change clocking is accomplished at a rate of 1 step every 8 ms or the 6 steps in 48 ms. Total time for the electrometer to reach 1 percent of a full scale step input in less than 1 second.

Gain accuracy is limited by the 10^{10} ohm electrometer resistor which has an initial accuracy of ± 2 percent and a temperature coefficient of 0.1 to 0.15

percent/C. An internal calibrator is provided which allows determination of the system gain to 1 percent at approximately 1×10^{-11} A.

Absolute accuracy of the electrometer system is limited by amplifier voltage and current offsets. Voltage offsets will be set to zero $\pm 5 \times 10^{-15}$ A reference to the input initially. Current offset has not been guaranteed by the FET manufacturer but it should be reasonable to expect it to be an order of magnitude better than the guaranteed leakage which would yield 2×10^{-14} A at 25C. The breadboard electrometer demonstrated an offset current of 1.5×10^{-14} A with bias currents at the inverting and noninverting inputs being 2.4 and 3.75×10^{-14} A respectively at 25C. The offset increased to 8×10^{-14} A at +40C.

The temperature coefficient of the breadboard electrometer was approximately 7×10^{-15} A/C over the temperature range of -20C to +50C.

An inflight electronics calibration is performed by sending pulses at a known rate and height through the discriminators into the four individual counting circuits of the SEM system; whereas known reference currents are injected into the electrometer circuits.

Geophysical Data

The ESUM experiment is designed to make absolute radiometric measurements of the solar irradiance and its temporal variations in the EUV to an accuracy of 5 to 10% through the use of synchrotron radiation as an absolute standard of irradiance. A fundamental limitation on the accuracy of broad band radiometry is that one must assume that one knows the distribution of irradiance within the pass band of the photometer channel except for a constant factor.

The calculated signal from a particular combination of aperture, neutral density filters, metallic filter, and detector is

$$S(\text{calc}) = \text{ATR}(\theta, \phi) \sum_{\lambda_i} f_{\lambda_i} \Delta \lambda_i t_{\lambda_i} Q_{\lambda_i}$$

The signal observed is

$$S(\text{Obs}) = \text{ATR}(\theta, \phi) \sum_{\lambda_i} F_{\lambda_i}^*(\text{true}) \Delta \lambda_i Q_{\lambda_i}$$

Where A is the geometrical aperture,

T is the combined transmittance of the neutral density filters,

R(θ, ϕ) is the angular response which is assumed to be independent of λ for small θ, ϕ .

F_{λ_i} is the model value for the solar irradiance at λ_i

F_{λ_i} is the derived solar irradiance from the ESUM experiment, t_{λ_i} is the metallic filter transmittance at λ_i

Q_{λ_i} is the detector quantum efficiency at λ_i

$\Delta \lambda_i$ is the wavelength interval, $t_{\lambda_i} \Delta \lambda_i$ is solar flux within the interval $\Delta \lambda_i$.

As previously stated one must assume that $n_{\lambda_a} f_{\lambda_i} = F_{\lambda_i}$ over the passband channel α .

The effective wavelength, λ_a , is defined as:

$$\lambda_a = \sum_{\lambda_i} (f_{\lambda_i} \Delta \lambda_i) (t_{\lambda_i} Q_{\lambda_i}) (\lambda_i) / \sum_{\lambda_i} (f_{\lambda_i} \Delta \lambda_i) (t_{\lambda_i} Q_{\lambda_i})$$

For the ESUM experiment there will be six weighting or normalization functions,

$\eta_{\lambda_a}(\tau)$, $\alpha = 1-6$, where τ is the variable of time. Once per day a model of the

EUV solar irradiance will be updated from the ESUM observations. In the ESUM derivation of the solar irradiance one assumes a linear interpolation is valid between $\eta_{\lambda_{\alpha}}$ and $\eta_{\lambda_{\alpha+1}}$ over the average of $\alpha = 1-6$.

Based on the ESUM observations the solar irradiance at any wavelength, λ_i , is $F_{\lambda} = \eta_{\lambda} f_{\lambda}$ where

$$\eta_{\lambda} = \eta_i + \frac{(\eta_{i+1} - \eta_i)}{(\lambda_{i+1} - \lambda_i)} \lambda.$$

Summary

The ESUM experiment has the potential of being able to do absolute photometry of the sun to an absolute accuracy approaching 5%, provided that the potentially harmful effects of contamination can be suppressed. Furthermore, the absolute basis is related to a laboratory radiation standard which can be derived theoretically. The absolute accuracy of the measurement of the EUV solar irradiance is dependent upon the degree of accuracy with which the relative solar energy distribution is known within the pass bands of the ESUM channels. The geophysical data which the ESUM experiment can provide for the Aeronomy Team will be a time dependent model of the solar irradiance in the EUV.

REFERENCES

1. Samson, James A. R., Techniques of Vacuum Ultraviolet Spectroscopy; John Wiley & Sons, Inc., New York.
2. Steele, Gordon N. and Reynolds, Wendell R., XUV Filter Development for the Extreme Solar Ultraviolet Monitor, Contract No. NAS 5-23082.
3. Hinteregger, Hans E., The Extreme Ultraviolet Solar Spectrum and Its Variation During a Solar Cycle, Ann. Geophys., 26, 547, 1970.
4. Rustgi, O. P., Study on a Technique for Detecting Photons in the 100-1000A Wavelengths Region, NASA CR-1096, 1968.
5. Schwinger, Julian, On the Classical Radiation of Accelerated Electrons, Phys. Rev., 75, 1912, 1949.
6. Tomboulion, D. H., and Hartman, P. L., Spectral and Angular Distribution of Ultraviolet Radiation from the 300-MeV Connell Synchrotron, Phys. Rev., 102, 1423, 1956.

Table 1

The ESUM Filters and the Wavelength Response Band
for 50% of the Signal Are Given

Filter	Detector	50% Signal Interval
1. Aluminum + Parylene	Channel	45-65A
2. Aluminum + Carbon	Channel	240-303A
3. Aluminum	Channel, Diode	270-550A
4. Titanium	Channel	365-535A
5. Tin	Channel	570-584A
6. Indium	Channel, Diode	800-935A
7. No filter	Diode	1216A

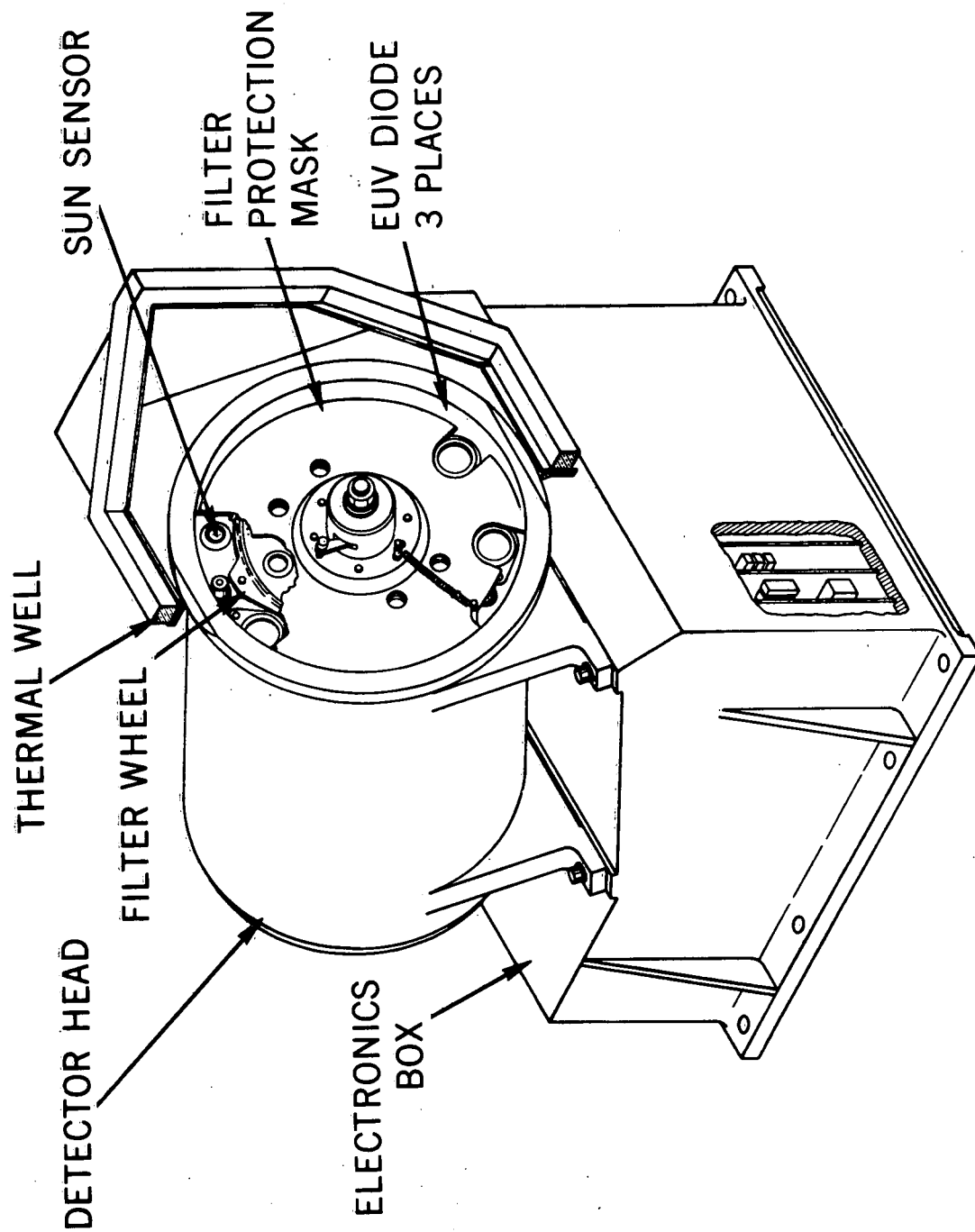


Figure 1. ESUM Experiment

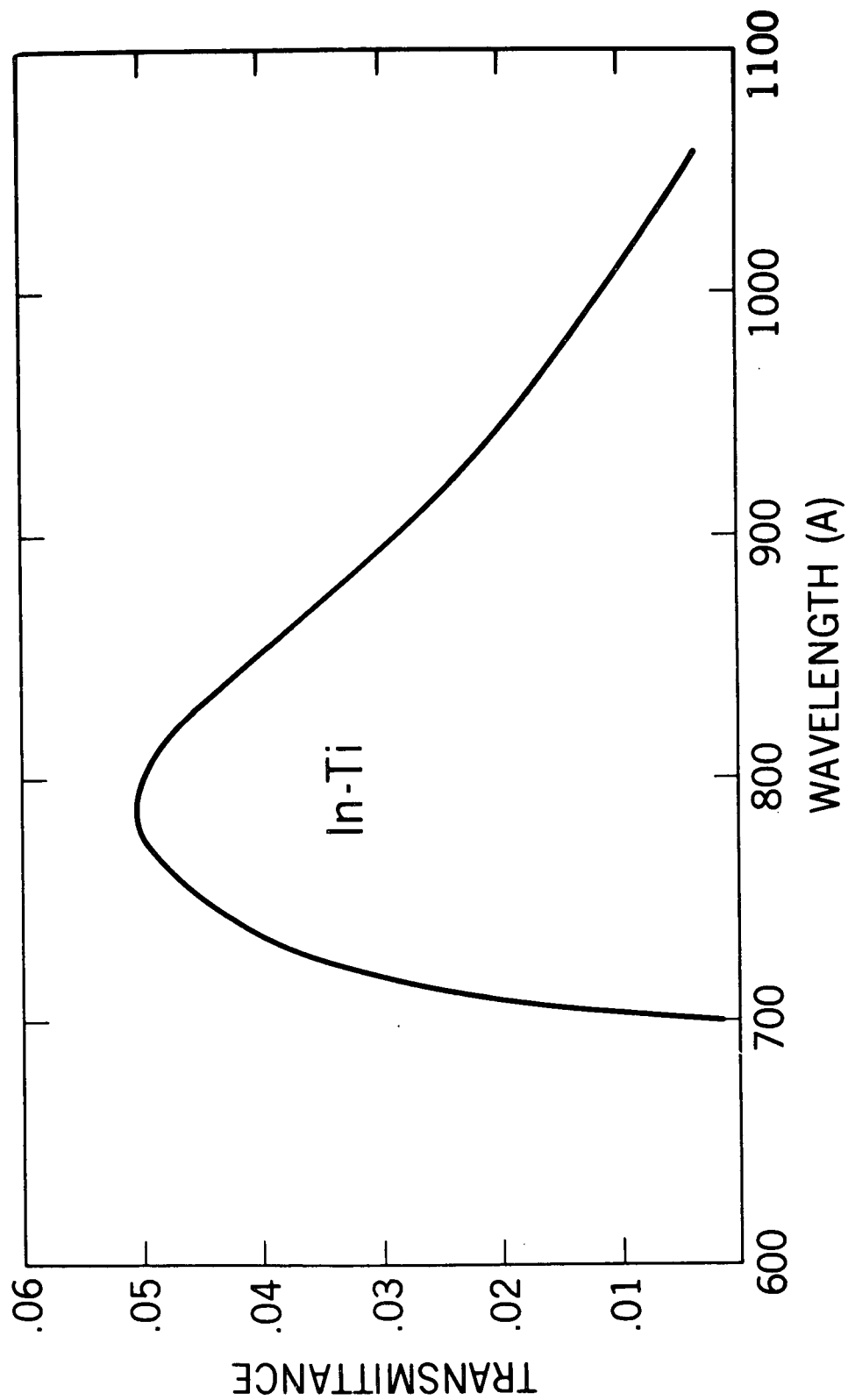


Figure 2. Transmittance for the 1730Å thick In - 1% Ti alloy filter shown here is comparable to a Sigmatron pure In filter of similar thickness.

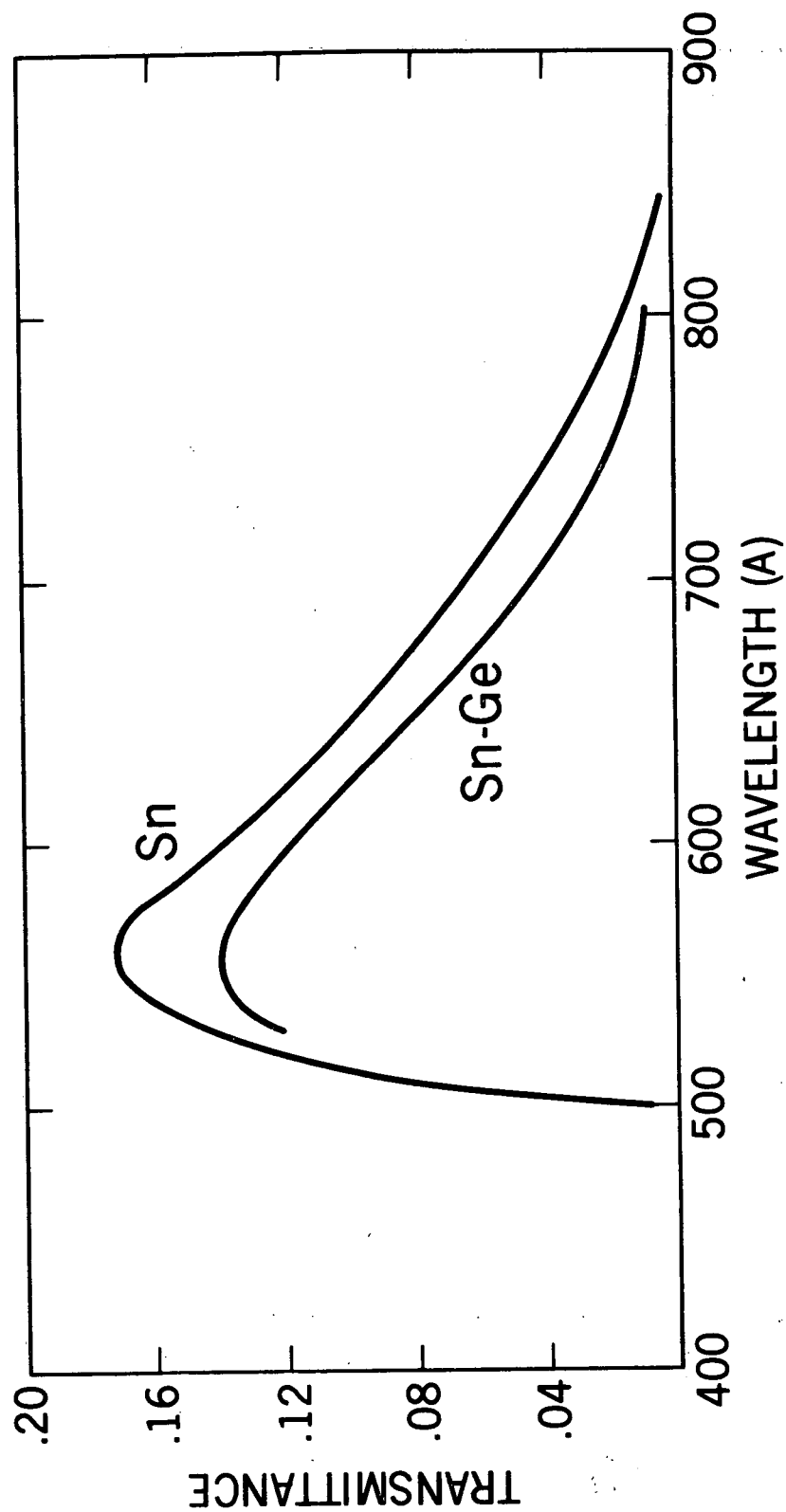


Figure 3. Comparison of the transmittances for a pure Sn filter (1600Å thick) and a Sn - 3% Ge (1700Å thick) alloy filter. The alloy filter exhibits superior resistance to moisture attack.

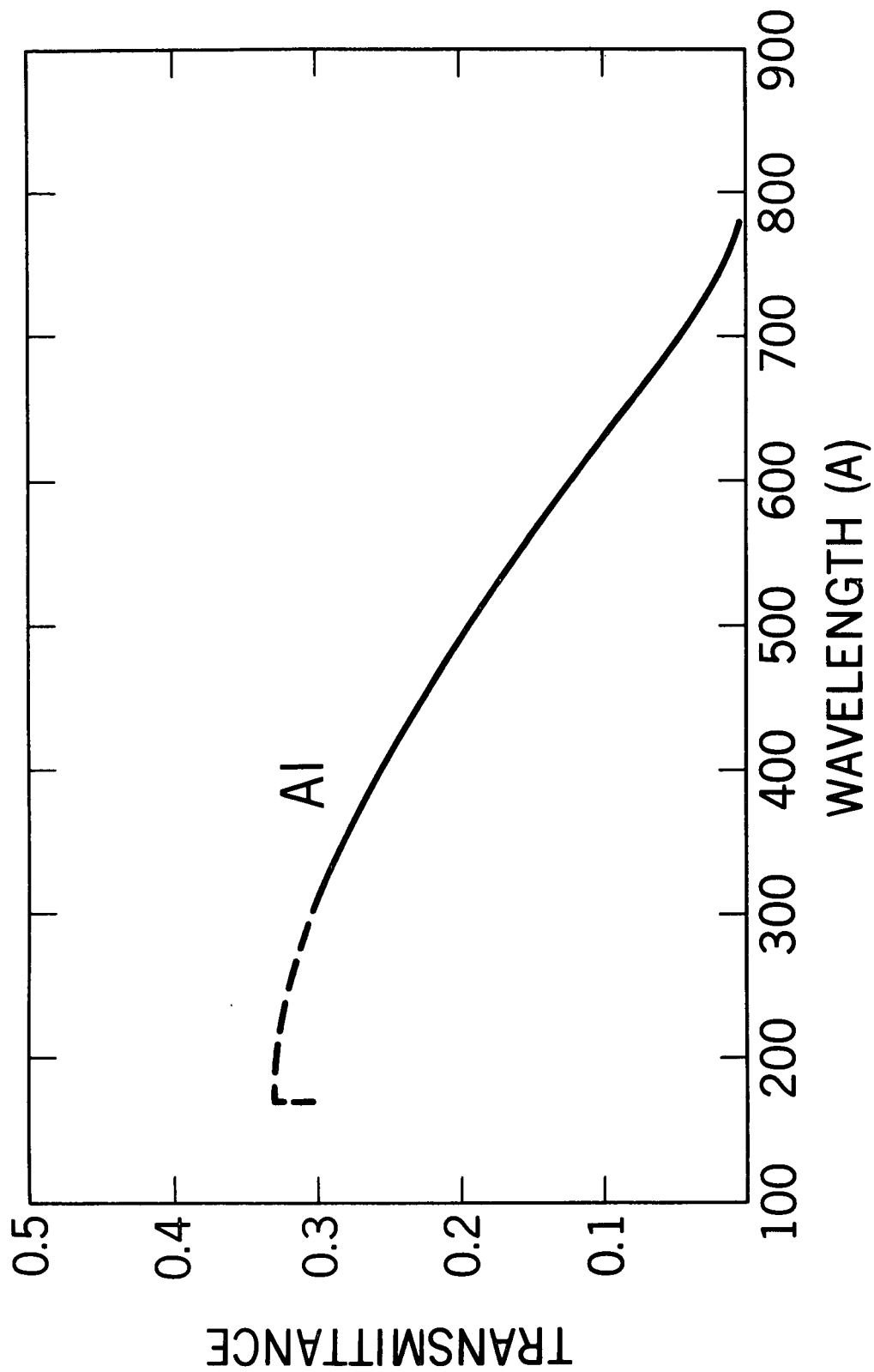


Figure 4. Transmittance for a standard sigma Al - 1% Si alloy filter 1800Å thick.

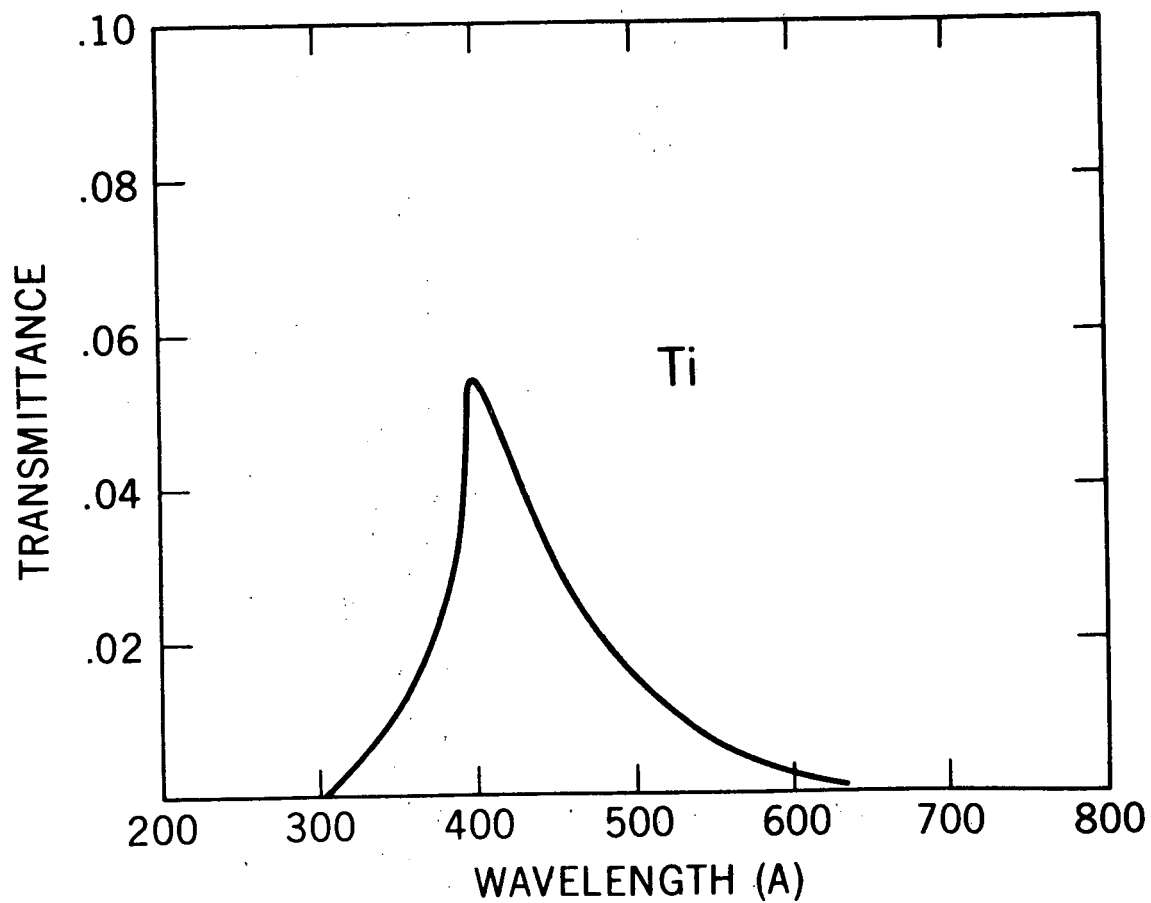


Figure 5. Transmittance for a 1000Å thick pure Ti filter which was pin-hole free but not opaque to visible radiation.

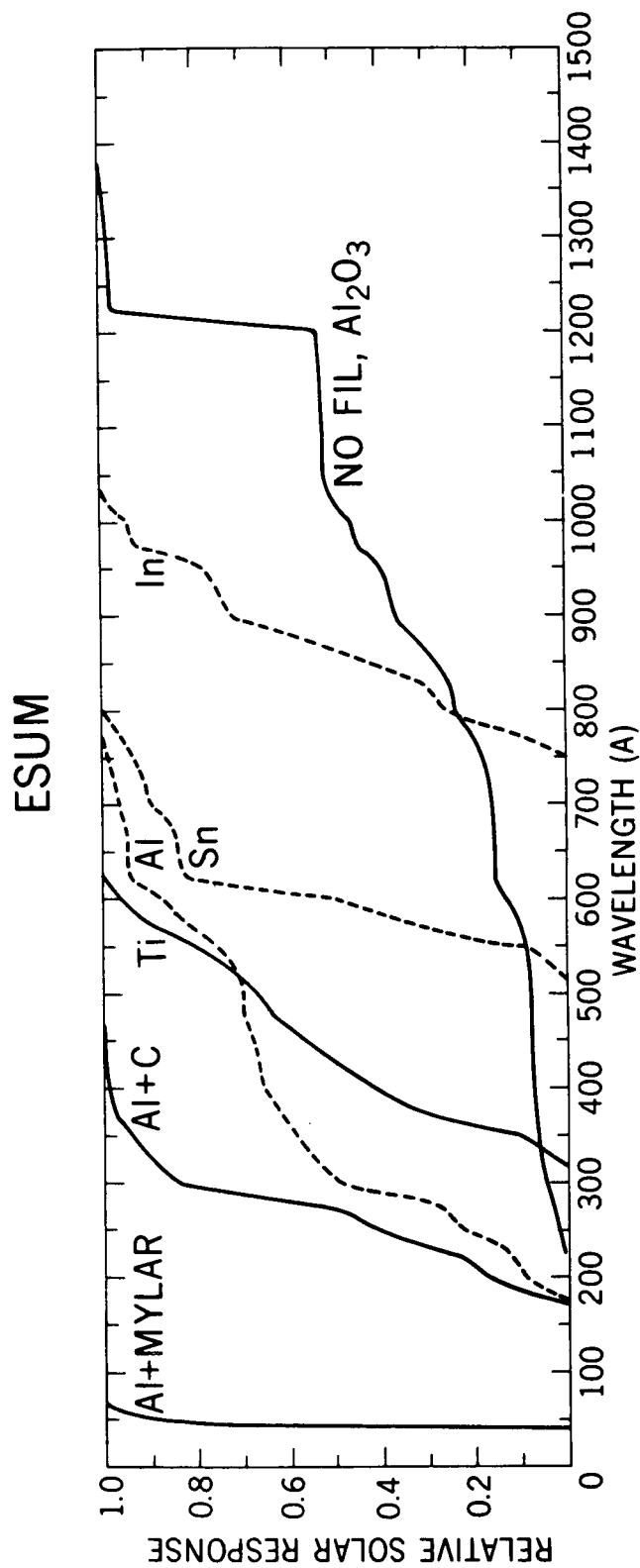


Figure 6. Calculated response of typical ESUM photometer channels using published filter transmittance curves and the NBS Al₂O₃ standard diode quantum efficiency curve depicted in Figure 7.

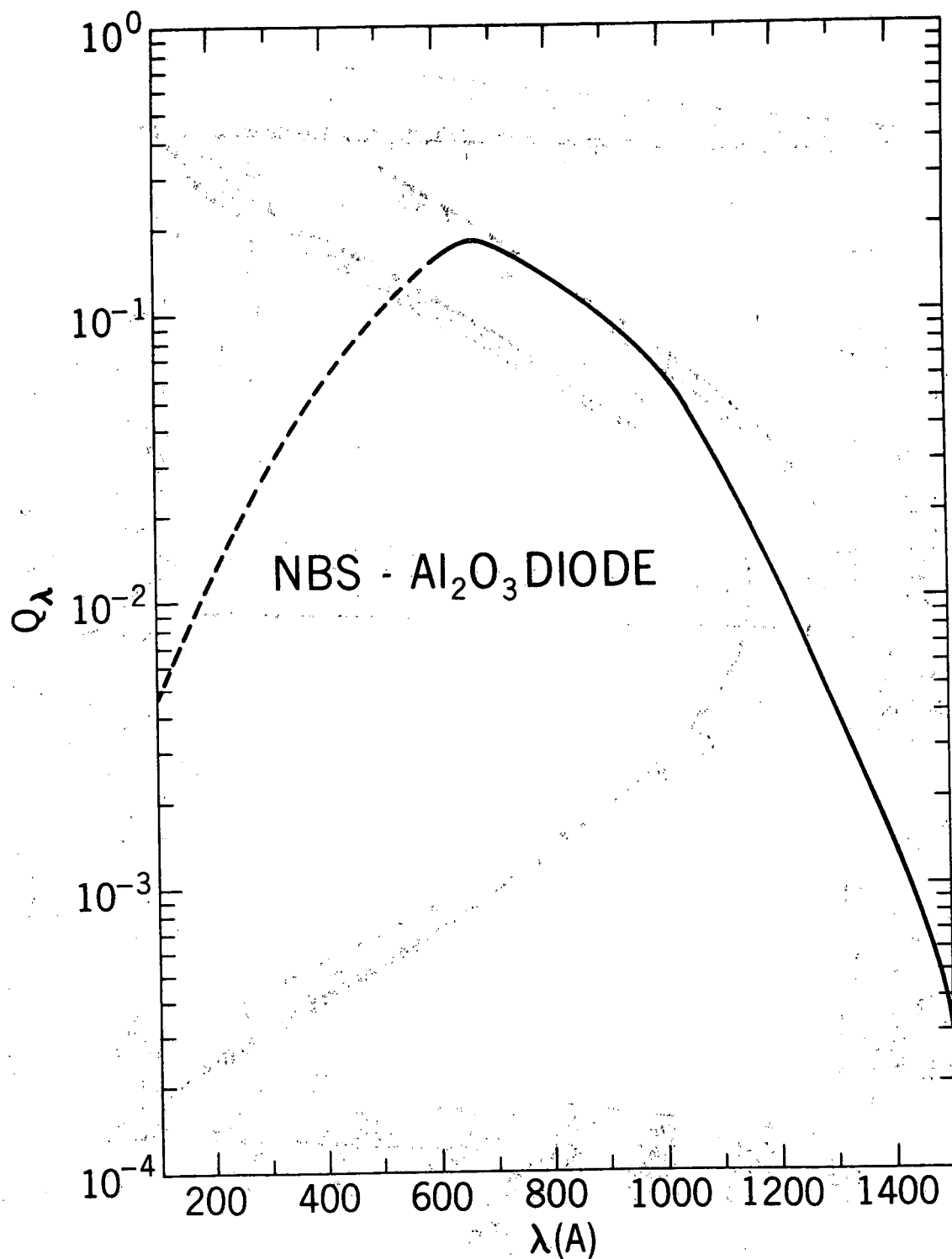


Figure 7. Quantum efficiency of NBS, Al_2O_3 standard diode. The broken curve below 600 \AA is an extrapolation some preliminary measurements (made at Ball Bros. Res. Corp.) indicate a plateau in quantum efficiency between 500 \AA and 200 \AA .

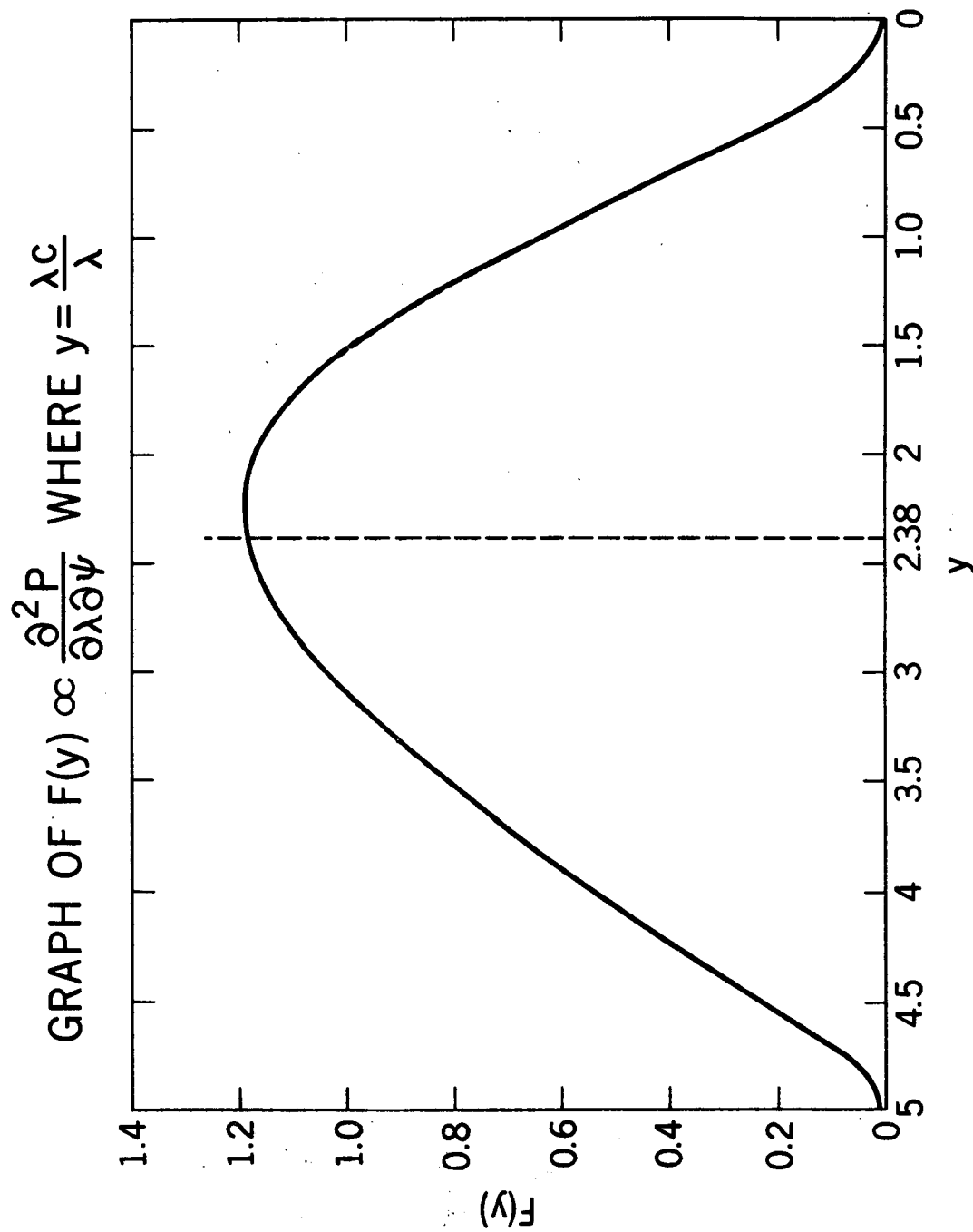


Figure 8. The function, $F(y) \propto \frac{\partial^2 P}{\partial \lambda \partial \psi}$ is the spectral distribution function where $y = \lambda c / \lambda$ and is used in the calculation of the emitted power per unit wavelength and angle.

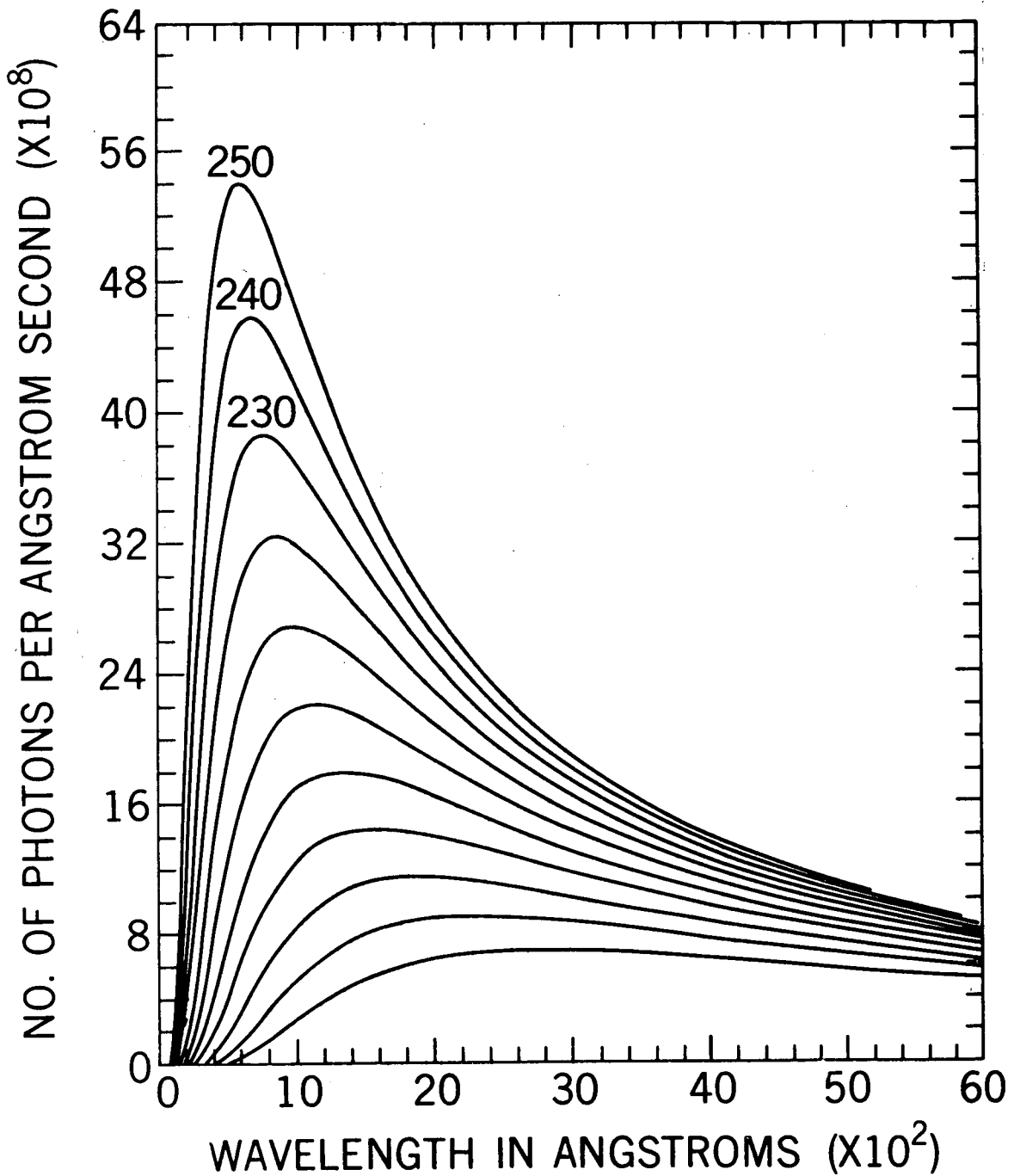


Figure 9. Spectral energy distribution for a 250 MeV, one milliamperere beam into one milliradian. The succeeding smaller curves are for decreases in energy in increments of 10 MeV.